Published in final edited form as:
J Neurochem. 2010 November ; 115(3): 716–734. doi:10.1111/j.1471-4159.2010.06970.x.

Subcellular Rearrangement of Hsp90-binding Immunophilins Accompanies Neuronal Differentiation and Neurite Outgrowth

H. Ramiro Quintá[*], **Darío Maschi**[†], **Celso Gomez-Sanchez**[‡], **Graciela Piwien-Pilipuk**[*], and **Mario D. Galigniana**[*,§]

[*] Instituto de Biología y Medicina Experimental/CONICET, Buenos Aires, Argentina

[†] IIBBA/CONICET, Buenos Aires, Argentina

[‡] Division of Endocrinology, G.V. (Sonny) Montgomery VA Medical Center and The University of Mississippi Medical Center, Jackson, MS, USA

[§] Departamento de Química Biológica, Facultad de Ciencias Exactas y Naturales, Universidad de Buenos Aires, Argentina

Abstract

FKBP51 and FKBP52 are TPR-domain immunophilins belonging to the TPR-protein hsp90 hsp70 p23 heterocomplex bound to steroid receptors. Immunophilins are related to receptor folding, subcellular localization, and hormone-dependent transcription. Also, they bind the immunosuppressant macrolide FK506, which shows neuroregenerative and neuroprotective actions by a still unknown mechanism. In this study, we demonstrate that in both, undifferentiated neuroblastoma cells and embryonic hippocampal neurons, the FKBP52•hsp90•p23 heterocomplex concentrates in a perinuclear structure. Upon cell stimulation with FK506, this structure disassembles and this perinuclear area becomes transcriptionally active. The acquisition of a neuronal phenotype is accompanied by increased expression of βIII-tubulin, Map2, Tau-1, but also hsp90, hsp70, p23, and FKBP52. During the early differentiation steps, the perinuclear heterocomplex redistributes along the cytoplasm and nascent neurites, p23 binds to intermediate filaments and microtubules acquired higher filamentary organization. While FKBP52 moves towards neurites and concentrates in arborization bodies and terminal axons, FKBP51, whose expression remains constant, replaces FKBP52 in the perinuclear structure. Importantly, neurite outgrowth is favored by FKBP52 overexpression or FKBP51 knockdown, and is impaired by FKBP52 knock-down or FKBP51 overexpression, indicating that the balance between these FK506-binding proteins plays a key role during the early mechanism of neuronal differentiation.

Keywords

FKBP; TPR proteins; Chaperones; p23; Tau; Hippocampus

Introduction

Immunophilins (IMMs) are a family of proteins that bind immunossupressive drugs and possess *cis/trans* peptidyl-prolyl-isomerase activity. They are classified as FKBPs (FK506-binding protein) when they bind FK506, and CyPs (cyclophilins) when they bind cyclosporine A (Pratt et al. 2004a). FKBP51 and FKBP52 (gene names *FKBP5* and *FKBP4*,

Correspondence should be addressed to: Dr. Mario D. Galigniana, Departamento de Química Biológica, Pabellón II, Facultad de Ciencias Exactas y Naturales, Ciudad Universitaria (C1428EGA), Buenos Aires, Argentina. mgali@qb.fcen.uba.ar.

respectively) are highly homologous tetratricopeptide (TPR)-domain immunophilins whose sequences share 60% identity and 75% similarity. The best characterized interactions of FKBP52 and FKBP51 are with hsp90 and steroid receptor complexes. It has been shown that FKBP52 is required for dynein/dynactin-dependent retrograde movement of glucocorticoid receptor (GR) (Galigniana et al. 2004b), mineralocorticoid receptor (MR) (Piwien Pilipuk et al. 2007), p53 (Galigniana et al. 2004a), RAC3 and AIF (Colo et al. 2008), and adeno-associated virus 2 (Zhao et al. 2006). Moreover, FKBP52 was found associated to androgen receptor (Cheung-Flynn et al. 2005), progesterone receptor (Kosano et al. 1998), estrogen receptor (Ratajczak and Carrello 1996), epithelial calcium channels (Gkika et al. 2006), and transient receptor potential (TRPC) channels (Sinkins et al. 2004). On the other hand, FKBP51 does not bind dynein (Wochnik et al. 2005) and shows inhibitory action of steroid receptor function, an effect that is abrogated by mutations of the TPR domain. This suggests that the association with hsp90 is relevant for that biological property.

IMMs are also present in the brain at higher concentrations than in immune cells (Snyder et al. 1998). The Bruce Gold laboratory found that the IMM-binding drug FK506 (Tacrolimus) shows neurotrophic effect (Gold et al. 1999) and it was initially thought that this effect involved calcineurin inhibition. However the persistence of the capability to hasten nerve outgrowth by FK506-derivatives devoid of immunosuppressive effects indicated that both effects are independent (Gold and Villafranca 2003). Experiments with mice where the *FKBP1A* gene was knocked-out clearly showed that such neurotrophic effect is not mediated by FKBP12, whereas the use of a monoclonal antibody against FKBP52 completely blocked the effect of FK506 (Gold et al. 1999). Even though this evidence suggests that FKBP52 could play a cardinal role in neuritogenesis, the molecular mechanism involving IMMs in neuronal differentiation and neurite outgrowth still remains totally unknown and there are no systematic studies to elucidate the cellular events related to this conundrum. In this study we analyzed the subcellular redistribution of the FKBP52•hsp90•p23 heterocomplex in undifferentiated N2a neuroblastoma cells and rat embryonic hippocampal neurons stimulated with FK506, and reveal for the first time some of the subcellular events involving these chaperones during the differentiation process of neurons.

Experimental procedures

Materials

FK506 and cyclosporine A (CsA) were from LC laboratories (Wobrun, MA). Radicicol, dibutyryl-cAMP, IBMX (3-isobutyl-1-methylxanthine), cycloheximide (CHX), α-amanitin, actimomycin D, H89 (N-[2-(p-Bromo-cinnamylamino)-ethyl]-5-isoquinoline-sulfonamide. 2HCl), dexamethasone (DEX), monoclonal IgM anti-vimentin (ascites), and mouse monoclonal IgG anti-β-tubulin were from Sigma Chemical Co. (St. Louis. MO). BuGR2 mouse monoclonal IgG against GR, JJ3 mouse monoclonal IgG against p23, and rabbit polyclonal IgG against FKBP51 were from Affinity BioReagents (Golden, CO). AC88 mouse monoclonal IgG against hsp90 and the N27F3–4 anti-72–73-kDa heat-shock protein monoclonal IgG (anti-hsp70) were from StressGen (Ann Arbor, MI). The purified UP30 rabbit antiserum against FKBP52 was provided by Dr. William Pratt (University of Michigan). The A3S rabbit monoclonal IgG against histone H3 and the rabbit polyclonal IgG against phospho-CREB were from Upstate (Temecula, CA). Rabbit polyclonal IgG against total CREB and goat anti-lamin B antibody were from Santa Cruz Biotech (Santa Cruz, CA). The HM-2 mouse monoclonal IgG against MAP2 and the horseradish peroxidase-conjugated goat anti-mouse were from Sigma Cemical Co. The TUJ1 mouse monoclonal IgG against neuronal class III β-tubulin was from Covance (Emerville, CA). Mouse monoclonal IgG against Tau-1 was from Chemicon (Temecula, CA). Rabbit polyclonal antibodies against ERK1/2 and phospho-ERK1/2, and the MEK inhibitor UO126

were from Promega (Madison, WI). Secondary antibodies labeled with Alexa-Fluor Dyes (488, 546 and 647) and TO-PRO-3 iodine were from Molecular Probes (Eugene, OR). Horseradish peroxidase-conjugated goat anti-rabbit was from Pierce (Rockford, IL). The siRNAs for FKBP51 and FKBP52 and control siRNA were purchased to Thermo Scientific Dharmacon (Chicago, IL). 5-Bromo-UTP was from Jena Biosciences (Germany), and rat monoclonal antibody against Br-uridine and mouse IgG anti-neurofilament were from Abcam (Cambridge, UK). All culture media were from Invitrogen-Life Technologies (Carlsbad, CA).

Cell cultures

N2a murine neuroblastoma cells were grown in DMEM/Opti-MEM (1:1) supplemented with 2 mM L-Gln, 5% fetal bovine serum (FBS) and antibiotics. N2a cell differentiation was initiated by serum withdraw and the addition of the indicated drug. 3T3-L1 preadipocytes were grown and differentiated to adipocytes by a standard procedure (Bennett et al. 2002). Hippocampal neurons were isolated from embryonic day 17 rat embryos (E17 cells) by a modification of a method described in the literature (Wang et al. 2002) (see legend of Suppl. 1 for details) and animal handling followed the procedures and ethic guides ruled by the University of Buenos Aires. Cell differentiation was stimulated the day after by adding the indicated compound to the medium. Neurite length was measured using the Image Pro Plus 5.1.0.20 program (Media Cybernetics Inc.) in those plate fields that showed low cell density.

Transfections

Overexpression of FKBPs was achieved by transfection of 1 μg DNA/well of 35 mm of either pCI-Neo-flag-hFKBP51, pCI-Neo-hFKBP52 or empty vector, following the calcium phosphate precipitation standard method (Gallo et al. 2007). Interference of FKBPs expression was achieved by transfection of the specific siRNA for each IMM (or an irrelevant siRNA) with the siImporter transfection reagent for RNA (Upstate, Temecula, CA) according to the manufacturer's instructions.

Indirect immunofluorescence assays

Cells grown on poly-lysine-coated coverslips were fixed and permeabilized as described (Galigniana et al. 1998). Fluorescence microscopy was performed in a Karl Zeiss LSM10 Meta confocal microscope. Image analyses for co-immunolocalizations were carried out using the 3D-surface plot plug-in of the Image-J program (v.1.42) from the NIH. 3D-Images were obtained from z-stack scanning of cells at a slice distance of 0.25 μm using the Imaris 6.3.1 program (Bitplane Sci Software, Zurich, Switzerland).

BrUTP-labeling of pre-mRNA

N2a cells were induced to differentiate for 6 h with 1μM FK506. Then, the coverslips were rinsed and incubated with 10 mM BrUTP in KH buffer (30 mM KCl, 10 mM Hepes at pH 7.4) for 7.5 min at 37°C under a 5%CO_2/95% air atmosphere. Cells were washed, reincubated in DMEM/10% fetal serum for 30 min, washed with PBS buffer, and fixed and permeabilized in cold (−20°C) methanol. Early mRNAs were visualized by indirect immunofluorescence with 1/100 dilution of rat monoclonal IgG antibody against Br-uridine. The specificity of pre-mRNA signal was tested by using a non-immune IgG antibody and after the inhibition of transcription with 100 μg/ml α-amanitin and 0.2 μg/ml actinomycin D as it is described in the literature (Jackson et al. 1993).

Data analysis

Results are shown as the mean ± SEM and were compared by unpaired Student's t test.

Results

Induction of cell differentiation

Neuronal differentiation was induced in mouse N2a neuroblastoma cells by serum withdrawal and addition of the compounds indicated in Fig. 1a, a procedure that restricted cell division and produced profound morphological transformations characterized by the outgrowth of neurites an axonal-like extensions. Fig. 1a shows the typical round shape of undifferentiated N2a cells was not affected by the vehicle (0.1% DMSO). One μM FK506 (a macrolide ligand able to bind to the FKBP subgroup of IMMs), 125 μM dibutyryl-cAMP (a classic neuronal differentiating agent), 0.2 μM radicicol (RAD) (a resorcylic acid lactone able to disrupt hsp90 function), and 10 nM cyclosporine A (CsA) (a cyclic non-ribosomal peptide that binds to the CyP subgroup of IMMs), were able to generate phenotypic changes as early as 1.5–2.0 h after adding the agent to the medium, FK506 and dibutyryl-cAMP being the inducers that generate the most dramatic changes in the cell shape in a medium without serum. Fig. 1b depicts the average neurite length of the cells as a function of the incubation time with the drug. Importantly, neither FK506 nor dibutyryl-cAMP showed toxic effects for the cells after 48 h of incubation, not even at the highest concentrations morphologic anomalies or neurite alterations were observed.

Visual inspection of the cultures after 2 h already showed that the cells exhibited longer neurites with FK506 or the cyclic nucleotide than cells incubated in the presence of the hsp90-inhibitor RAD or with CsA. The latter two compounds did show cytotoxic effects, so cells lost the incipient neuron-like morphology observed during the first hours acquiring a rounded shape and then, cells were detached from the plate. Those cells that remained attached exhibited shorter or null neurite length (Figs. 1a, 1b and Suppl.1b). Similar effects were also observed after 24 h with 4- to 5-fold lower concentrations of these compounds (Suppl.1b).

In all the cases, the frequent replacement of the medium supplemented with drug showed no significant changes in the response of the cells, whereas the addition of 48–72 h aged conditioned medium containing FK506 to undifferentiated cells triggered cell differentiation as efficiently as medium containing fresh drug (Suppl.1a). This differentiating effect persisted as long as additional 48 h after the aged medium was used. All these controls indicate that during the assayed incubation times there is no significant degradation of FK506 or generation of toxic metabolites.

Fig. 1c shows comparative drug concentration-neurite length response curves for the two most active agents, FK506 and dibutyryl-cAMP, after 3 h (tringles), 24 h (squares) and 48 h (circles) of incubation. FK506 shows the most efficient effect on neurite length. Because incubations with cAMP should favor CREB phosphorylation, the relative effect of FK506 was compared with that of the cyclic nucleotide by Western blotting of cell lysates with anti-CREB and anti-phospho-CREB antibodies (Fig. 1d). While the overall expression of CREB is not affected by the drugs, there are kinetic and quantitative differences between cAMP and FK506. Cells induced to differentiate with cAMP increased the phosphorylation of CREB. On the other hand, phosphorylation of CREB was negligible after 3 h with FK506, but it was intense in cells stimulated for 24 h with FK506. Such difference suggests that the molecular mechanisms of action of the IMM ligand and the classical neurotrophic compound are not equivalent, in particular if it is considered that CREB phosphorylation takes place after 3 h of stimulation with cAMP, but it remains unchanged with FK506.

Fig. 1e shows Western blots of N2a cell lysates for typical markers of neuron differentiation. After stimulation with dibutyryl-cAMP or FK506, these markers were induced accompanying the morphological changes of the cells. There was a strong induction of βIII-

tubulin, a neuronal microtubule isoform that is considered to be one of the earliest markers to signal neuronal commitment. Also, there was a strong induction of Tau-1, a typical axonal marker, as well as all three isoforms of the primarily dendritic microtubule-associated protein 2 (Map 2a, 2b and 2c), being of particular relevance the 70-kDa isoforms Map-2c because it is present in the early steps of cell brain morphogenesis (Tucker 1990).

TPR-domain immunophilins bind FK506 and form heterocomplexes with other chaperones that are required for remodeling the architecture of cytoskeletal structures (Czar et al. 1996; Galigniana et al. 2002; Chambraud et al. 2007; Inberg et al. 2007), a process that should be a necessary step to underlie the neurite extension rate. When N2a cells were induced to differentiate for 48 h, hsp90, hsp70, FKBP52 and p23 were greatly induced (Fig. 1e). On the other hand, FKBP51 remained unchanged. Consistent with the results described in the other panels, FK506 showed to be more efficient to induce these chaperones, in particular the triad of the 90-kDa heat-shock protein and the hsp90-binding partners FKBP52 and p23.

FK506 effect differs from the cAMP action and hsp90-related pathways

To study whether or not there are additive, synergistic or antagonistic effects between some of the drugs assayed in Fig. 1, undifferentiated N2a cells were stimulated with FK506 in the presence of IBMX or RAD. Fig. 2a shows the mean neurite length for control experiments where the response of the cells to each treatment was analyzed during the first 24 h of stimulation. The mean neurite lengths obtained with each drug reproduced those measured in Fig. 1. Because most of the neurotrophins exert their effects via the cAMP pathway, phosphodiesterase inhibitors are broadly used as neurotrophic and neuroprotective agents (Castren 2004). IBMX was assayed to induce higher levels of endogenous cAMP, such that 500 μM of phosphodiesterase inhibitor generated equivalent neurite length after 48 h as that obtained with exogenous cAMP after 24 h. However, IBMX inhibited FK506 effect on neurite outgrowth by about one third of the maximum effect observed with FK506 alone. Similarly, the inhibition of hsp90 by RAD showed 50% of the maximum effect of the IMM drug. This observation indicates that the FK506 effect needs active hsp90-dependent pathways. It should be pointed out that similar qualitative results were obtained after 24 h of incubation, although the absolute values were obviously smaller (Suppl. 2).

Another important phenotypic change observed in the cells was the number of ramifications per cell (Fig. 2b), which was significantly higher with radicicol alone (3 vs 2 neurites/cell) compared to FK506 or IBMX alone. Even though FK506 and IBMX together showed a lesser efficient neurite outgrowth than cells incubated with FK506 alone, both drugs added their individual effects when the number of ramifications was counted (4 neurites/cell). On the other hand, FK506 showed antagonistic action on the effect of the hsp90 inhibitor, suggesting that the inhibition of IMM activity abrogates the hsp90-dependent effect on branching. In short, hsp90 is an important requirement (although not exclusive) for neuronal arborization, whereas IMMs are factors more related to the neurite length.

The effects of both glucocorticoids and hsp90 inhibitors on neurite outgrowth led to speculate that steroid receptors may be involved in the mechanism of action of the neuritogenesis phenomenon (Gold 2000; Gold and Villafranca 2003). The expression of the GR during the development of the nervous system (and also in cell cultures) seems to be sensitive to several regulations, and conflicting results have been reported on the effects of glucocorticoids on neurons (Wang et al. 2002; Xiao et al. 2005). It has recently been reported that at different developmental stages, hippocampal neurons show different susceptibilities to glucocorticoids influenced by environmental changes and there might be a critical time-window for the switching of such characteristics during development (Xiao and Chen 2008). Because our cells are originally grown in a medium containing serum, they are consequently exposed to glucocorticoids. Therefore, we analyzed the potential influence of

glucocorticoids on the FK506-dependent neurite outgrowth. Cells were grown in a steroid-free medium for 24 h to deplete traces of steroid. Next, the cells were preincubated for 30 min with 1 μM dexamethasone to allow binding of the agonist to GR and then, 1 μM FK506 was added to the medium to trigger cell differentiation. Fig. 2c shows that after 24 h, N2a cells adopted identical neuron-like phenotype as control cells maintained in steroid-free medium. Accordingly, Fig. 2d shows identical expression of the neuronal markers βIII-tubulin y Map-2. In other words the mechanism of action of the IMM ligand is not directly related to GR.

Subcellular distribution of the FKBP52•hsp90•p23 complex

Our results demonstrate for the first time that the expression of FKBP52, hsp90 and p23 is increased during neuronal differentiation (Fig. 1e), suggesting a potential role for these chaperones during the process. Therefore, their subcellular distribution was analyzed by confocal microscopy. Surprisingly, images of undifferentiated cells showed that all three proteins are concentrated in a perinuclear ring (Fig. 3a). After 3 h of treatment with FK506, the chaperone complex was dispersed in cell cytoplasm and no visible arrangement was detected. Shorter incubations with FK506 (1 h) demonstrate that the disassembly of the annular structure is an early event and is also sequential because p23 could still be seen as a perinuclear ring when FKBP52 and hsp90 were already dispersed into the cytoplasm. More than 95% of undifferentiated cells show the chaperones colocalizing in a perinuclear structure, whereas only 20% of the cells show a full perinuclear ring after 3 h with FK506, indicating that chaperones migrate rapidly and spread out in the cytoplasm and neurites. This is evident in Fig. 3a for hsp90 and FKBP52 in cells incubated for 1 h with FK506.

Note that cells showing incipient axon-like structures exhibit higher concentration of FKBP52 in the growth cones and on the extremes of the neurites, a feature that was exacerbated after 24 h when the cell body has already acquired a typical neuronal phenotype. While FKBP52, hsp90 and p23 colocalized in perinuclear structures in undifferentiated cells, they rather show a dissociated localization in the arborization bodies and terminal ends of the neurites. In a high number of cells, FKBP52 concentrates in the central part of the structure being surrounded by hsp90 and p23. Fig. 3b shows a magnification of a ramification body. Because these bodies are found in areas of neurite arborization and at the leading growing extremes of neurites, we hypothesize that these chaperones may be involved in the reorganization of the cytoskeleton, which is expected to be highly dynamic in these structures.

Fig. 3c shows that the peculiar organization of nuclear FKBP52, hsp90, and p23 observed in N2a cells is not exclusive of this neuronal cell line because all three proteins also redistribute from the perinuclear ring to the cell body and the neurites upon treatment with FK506 in hippocampal neurons isolated from 17 days rat embryos. In similar fashion as in N2a cells, there is a high percentage of cells where FKBP52 concentrates in growth cones of outgrowing neurites and at the nascent neurites (Fig. 3d).

To analyze whether the chaperone complex concentrates in perinuclear rings in any undifferentiated cell, 3T3-L1 preadipocytes were also analyzed in conditions where adipocyte differentiation is not triggered. Fig. 3e shows that p23, FKBP52 and hsp90 have a predominantly diffuse subcellular distribution pattern. Note that hsp90 shows a slight perinuclear rim, although it is less intense than that exhibited in the rings of neuronal cells. This is an expected distribution for hsp90, which is associated to nucleoporins (Echeverria et al. 2009;Galigniana et al. 2010) and microtubules that curl up around the nucleus in epithelial cells (Czar et al. 1996). No differences in the subcellular distribution pattern of all three proteins was observed when 3T3-L1 cells are induced to differentiate with a standard differentiation cocktail composed by IBMX, dexamethasone and insulin (Suppl.3).

We have performed immunoprecipitation assays and have found that, as it is expected for this hsp90-based complex (Murphy et al. 2003), all three proteins co-immunoprecipitate. However, this type of assay cannot distinguish between the highly abundant FKBP52•hsp90•p23 complexes normally present in cytosol from those heterocomplexes located in annular structures. Nonetheless, there is no reason to think that complexes cannot be formed and we assume that all three proteins in the perinuclear ring may assemble in the same type of heterocomplex found in soluble cytosol, as it has been profusely demonstrated for many other systems (Freeman et al. 2000; Galigniana et al. 2001; Sullivan et al. 2002; Pratt et al. 2004b; Colo et al. 2008). To provide evidence that these chaperones may form a complex in the nuclear ring, an indirect immunofluorescent was performed for hsp90 using the mouse IgG clone AC88, which recognizes free and denatured chaperone, but it is unable to react with hsp90 when the chaperone is complexed (Galigniana 1998). Fig. 4a shows that FKBP52 forms a ring in undifferentiated cells, but hsp90 cannot be detected as it is with the IgM clone 8D3 used in Figs. 3 and 4b. Therefore, the hsp90 belonging to the perinuclear ring is part of a complex. Unfortunately, p23 cannot be seen along with FKBP52 because the antibody is also a mouse IgG and the rabbit IgG variant against p23 is not useful for indirect immunofluorescence assays.

A recent study demonstrated that growth cone responses require synthesis of proteins. However axonal elongation continues when protein synthesis inhibitors are added before cue agents are added to the medium (Roche et al. 2009). To study whether or not protein synthesis is strictly required for the mechanism of ring disassembly and neuron differentiation, N2a cells were preincubated for 30 min with 20 nM cycloheximide (CHX). Then, the medium was replaced by DMEM supplemented with FK506 and CHX. After 3 h, cells were fixed and stained for p23, hsp90 and FKBP52. Fig. 4b shows that the perinuclear ring was unaffected by the preincubation with CHX (compare −CHX vs +CHX). After 3 h with FK506 (and the continuous presence of CHX), the cell shape changed similarly to untreated cells, and hsp90 and FKBP52 abandoned the perinuclear structure as it was observed in Fig. 3. However, p23 remained in the nucleus of all cells. This indicates that the population of hsp90 and FKBP52 that normally expands into the cytoplasm when cell differentiation is triggered represents a pre-existing pool of chaperones rather than protein synthesized *de novo*, which is also confirmed by the Western blot for chaperones shown in Fig. 4c. On the other hand, these results suggest that p23 relocalization may depend on the synthesis *de novo* of some additional factor required for delocalizing the co-chaperone from the ring. This could explain why p23 abandons the perinuclear structure at latter times than hsp90 and FKBP52 and also emphasizes the importance of these chaperones in the early steps of neuronal differentiation. We will address the importance of FKBP52 for ring assembly in experiments shown later on.

The FKBP52•hsp90•p23 complex is intranuclear

Next, we asked whether the ring of chaperones on the nuclear periphery is inside the nucleus or it is associated to cytoskeletal filaments coiled-up around the nuclear envelope. Fig. 5a shows that the ring of chaperones is inside the nucleus located immediately under the nuclear envelope (see the borders of the envelope pointed by yellow arrowheads). This is confirmed in Fig. 5b, where it is shown the colocalization of chaperones with B-type lamin. Moreover, the upper right corner of Fig. 5c shows an indirect immunofluorescence for p23 (green) in cells whose nuclei were stained with the DNA probe TO-PRO-3 iodine (red). The resultant yellow ring agrees with the intranuclear localization of the protein. The computer generated 3D-image obtained from a z-stack scanning of the cell confirms that the yellow ring is inside the nucleus (note the black arrow pointing the red area of chromatin that surrounds the annular structure).

The colocalization of chaperones with B-type lamin observed in Fig. 5b for N2a cells was also seen in primary embryonic hippocampal neurons (Fig. 5d), indicating that the annular structure is not a peculiarity of the cell line.

Activation of MAPK (ERK) pathway

Nerve growth factor and other members of the neutrotrophin family are important factors for neuron survival and differentiation (Santos et al. 2007; Willard et al. 2007). It is accepted that these trophic factors function via activation of the MAPK cascade, and it has been reported that FK506 potentiates NGF-induced neurite outgrowth via this pathway (Price et al. 2005). Nevertheless, the ability of this network to coordinate the differentiation process in neurons is still unknown. Because in our studies cells are induced to differentiate in a medium lacking serum, cells are not exposed to any trophic factor except FK506. Therefore, we analyzed whether the ERK cascade pathway is activated by FK506 alone and, more importantly, whether this eventual activation is related to the particular perinuclear distribution of chaperones described in this study.

Fig. 6a shows that FK506 induced the expected phenotypic modifications observed in Fig. 3, including the late trafficking of p23 towards the cell body and neurites. Importantly, the subcellular redistribution of chaperones was evident 30 min after the differentiation process was induced by FK506. Fig. 6b demonstrates that ERK is transiently phosphorylated during the early steps of FK506-dependent differentiation. The inhibition of ERK phosphorylation by the MEK inhibitor UO126 (whose efficiency is shown in the Western blot of Fig. 6b) abrogates both cell differentiation and the disassembly of the perinuclear ring (Fig. 6a). This indicates that one process is directly related to the other and not the mere consequence of the effect of the drug on, for example, inhibition of the PPIase activity of IMMs. It is important to emphasize that these cells were incubated in a serum-free medium prior the treatment, and then FK506 was added to the medium. This strengthens the observation that FK506 shows differentiating effects per se and it is not enhancing residual effects already triggered during the growing period in the presence of putative trophic factors present in the serum. In addition, the results show that FK506 promotes both the activation of ERK cascade and chaperone migration from the nuclear periphery.

Because cAMP also elicits neurite outgrowth (Fig. 1) and has been linked to ERK1/2 activation via PKA in neuronal differentiation pathways (Yao et al. 1998;Hansen et al. 2003;Hu et al. 2003;Consales et al. 2007;Yang et al. 2008), it was analyzed whether the activation of PKA is involved in the disassembly of the annular chaperone complex and the FK506-dependent neurotrophic effect. Fig. 6c shows that H89, a selective cell permeable PKA inhibitor, fully abrogates both cAMP-dependent perinuclear chaperone disassembly and neurite outgrowth, whereas it showed no effect on FK506-dependent action. These results clearly show that PKA activation is involved in neurite differentiation, but it is independent of the mechanism triggered by FK506. These clashing observations for cAMP and FK506 action agree with their dissociated properties in Figs. 1d, 1e, 2a and 2b, indicating that both compounds have different molecular mechanism of action.

Transcriptional activity in the perinuclear structures

In Fig. 5, B-type lamin was used as marker of the intranuclear area located next to the envelope. B-type lamin was chosen for this analysis rather than the other types of lamins because the expression of A- and C-types is developmentally regulated and may be absent in early embryonic states as it is also absent in certain stem cell populations in adults (Stewart et al. 2007). Nuclear lamina has important roles in regulating RNA transcription and in the organization of chromatin, and many transcriptional cofactors associate with lamins suggesting a potential role in transcriptional regulation (Schirmer and Foisner 2007).

Therefore, we analyzed whether the perinuclear ring observed in untransformed cells correlates with the transcriptional activity in the area where the chaperones are present. If chaperones participate directly or indirectly in the heterochromatization of genes normally observed next to the nuclear envelope, the annular area occupied by chaperones should show poor transcriptional activity, whereas the disassemble of the heterocomplex should reverse this condition. The visualization of early mRNAs labelled with Br-UTP is shown in Fig. 7. The perinuclear area of undifferentiated cells shows lower production of pre-mRNAs than cells treated with FK506, where the annular structure originally occupied by hsp90 and FKBP52 becomes more active transcriptionally, to the point that Br-uridine labeling itself forms a notable ring of early mRNAs. Even though we expected greater transcriptional activation in this area upon chaperone disassembly, such a highly concentrated transcriptional activity was totally unexpected. The specificity of the Br-uridine signal was tested using non-immune primary antibody and/or different secondary antibodies. In addition, the annular signal of RNAs was totally abolished after abrogating the transcriptional activity with α-amanitin and actinomycin D in FK506-trated cells. It should be pointed out that hsp90 and FKBP52 were colabeled with Br-uridine independently to exclude potential cross-reactions of the antibodies.

FKBP52 concentrates in axons

Because FKBP52 seems to be a key component of the heterocomplex during the differentiation process and is a target of FK506, we investigated the specific subcellular redistribution of this IMM in embryonic hippocampal neurons induced to differentiate with the immunosuppressant drug. FKBP52 was detected in the cell body and dendrites, but not in the axons unless neurons were incubated with FK506 (Fig. 8a). As expected, an indirect immunofluorescence for Tau-1 stained the cell body and axons of hippocampal neurons. Such redistribution of FKBP52 to axons was more clearly seen in cells immunostained for the dendrite marker Map-2 (Fig. 8b), whose signal is not detected in axons. Importantly, the presence of FKBP52 in axons correlated directly with a longer average length of the axons in FK506-treated hippocampal neurons compared with the length measured in untreated cells (Fig. 8c).

Cytoskeleton rearrangement

Figs. 3a, 4b and 6a show that p23 is the slowest protein to abandon the perinuclear ring upon cell stimulation with FK506. We noticed that in many cells, p23 locates in filamentary structures that are born next to or around the nuclear envelope. Therefore, we investigated the nature of those filaments. Fig. 9a shows that p23 does not colocalize with microtubules (upper panel) or microfilaments (lower panel), whereas Fig. 9b demonstrates a clear association of the co-chaperone with intermediate filaments, suggesting a role for p23 on their stabilization. The right panels are showing computer-generated 3D images of the filaments at the level pointed by the yellow arrow-head.

Figs. 3b and 3d emphasized the fact that when the heterocomplex is disassembled, its components concentrate in arborization bodies and terminal axons. Interestingly, the filamentary structure of microtubules and microfilaments is disrupted if p23 is concentrated in these cell structures, but this is not the case for the intermediate filaments where p23 is bound (Fig. 9c).

Interestigly, the cytoplasmic redistribution of all three chaperones accompanies a higher level of organization of microtubules, whose polymerization in undifferentiated cells (0 h) is surprisingly poor (Fig. 9d, left green panels). In these cells, tubulin staining is more evident around the nucleus (as it is normally seen in most cell types), but strong filaments are not evident, and the cytoplasm shows a relatively diffuse staining compared to the typical

filamentary net observed after cell incubation with FK506 for 3 h. On the other hand, phalloidin-labeled microfilaments do not show differences between both states of differentiation (Fig. 9d, red right panels). Taken together, these images agree with the fact that chaperone distribution along the cytoskeleton unquestionably parallels the reorganization of the cytoskeleton.

FKBP51 replaces FKP52 in the perinuclear ring

Of the FK506-binding protein family, FKBP51 has the highest homology with FKBP52 and shares similar crystallographic structures (Sinars et al. 2003). Therefore, the subcellular distribution of FKBP51 was studied and compared to that observed for FKBP52. Because we have always recovered hsp70 associated to FKBP51 in most of the previously assayed systems including N2a cells (see insert in Fig. 10a), the subcellular distribution of hsp70 was also studied.

Fig. 10a shows that, in contrast to the full annular structures observed for FKBP52 and hsp90, FKBP51 localizes along with hsp70 in fragmented bodies distributed randomly around the nucleus of N2a cells, although most frequently in the nuclear poles. When the cells were treated with FK506, this nuclear ‘capping’ appearance of FKBP51 and hsp70 was transformed into a defined full ring identical to that shown by FKBP52, hsp90 and p23 prior to the treatment.

The tight association of intermediate filaments with the nucleus and the isolation of crosslinkage products of them with genomic DNA fragments, including nuclear matrix attachment regions from proliferating cells, point to a participation of these filaments in nuclear activities (Tolstonog et al. 2002). Moreover, it has been reported that neurofilaments may be confined to the perinuclear zone during neuronal differentiation (Encinas et al. 2000; Shu et al. 2004; Ayala et al. 2007; Buttiglione et al. 2007). Because this phenomenon resembles FKBP51 relocalization, we analyzed the effect of FK506 treatment in the subcellular localization of endogenous FKBP51 along with neurofilaments. Fig. 10b shows that both factors were also concentrated in perinuclear rings. The lower panel shows that, in contrast to the redistribution of FKBP52 along the cell body and axons observed during the differentiation process (Fig. 8), FKBP51 remained mostly confined to the cell body and is recruited to perinuclear structures.

In view of the increased transcriptional activity acquired during the early steps of the differentiation by the nuclear area originally occupied by the annular structure of chaperones (Fig. 7), the possible involvement of FKBP51in those areas was also studied. Fig. 10c shows that when FKBP51 is recruited to the nuclear structures, it colocalizes with transcriptionally active nuclear domains.

FKBP51 antagonizes FKBP52 properties

Inasmuch as FKBP51 and FKBP52 are highly homologous IMMs that show antagonistic action in steroid receptor function (Wochnik et al. 2005), the possibility that both proteins may play an antagonistic role in neurite outgrowth was also explored. Fig. 11a shows that FKBP51 overexpression significantly impaired neurite outgrowth whereas FKBP52 overexpression enhanced neurite length. Furthermore, Fig. 10b shows that abrogation of FKBP51 expression with a specific siRNA accelerated neurite outgrowth after 4 h of treatment with FK506 with respect to controls. Actually, untreated cells already showed longer neurites (see black bar at zero time). These effects cannot be assigned to inhibition of the expression of FKBP52, a positive differentiating factor, since the expression of this IMM remained unchanged after knocking-down FKBP51 (Western blot is shown on the top of the bars). On the other hand, neurite outgrowth was abrogated in all the cells were the

expression of FKBP52 was silenced and the expression of FKBP51 remained unmodified (Fig. 10c).

In view of the fact that the formation of perinuclear rings of chaperones seems to be an important event related to neuronal differentiation, we also analyzed whether or not FKBP52 is essential for the formation of such structures. When N2a cells were transfected with specific siRNA to abrogate the expression of FKBP52 and the signal of the IMM was greatly decreased (see Fig. 10d, where the photography was overexposed to detect the fluorescence of FKBP52), neither hsp90 nor p23 were recovered in annular rings. Importantly, any of these cells developed neurites during the lapse of the experiment compared to FKBP52 expressing cells, suggesting that this IMM is essential for the efficient development of neurites. Therefore, FKBP52 appears to be a key factor related to neuronal differentiation and can be associated to the particular arrangement of chaperones in nuclear structures.

Discussion

Since the discovery that the immunosuppressant drug FK506 accelerates functional recovery and axonal regeneration in the rat sciatic nerve-crush model, the mechanism related to cell differentiation and neuritogenesis has remained enigmatic and not fully addressed to date. N2a neuroblastoma cell line and embryonic hippocampal E17 neurons provide a superb model to study molecular programs along differentiation. Here we show for the first time a very peculiar property of undifferentiated neuronal cells. The FKBP52•hsp90•p23 complex forms a perinuclear ring that undergoes a rapid subcellular redistribution along the cytoplasm, FKBP52 being concentrated in terminal axons and arborization areas. In agreement with the potential importance of this IMM inferred from its subcellular redistribution, knock-down experiments showed that FKBP52 play a key role in the architecture of these nuclear rings since these structures faded in most cells (if not all of them) where the expression of this IMM was abrogated (Fig. 11d). Importantly, both the rate of cell differentiation and neurite outgrowth were also inhibited.

There is a direct relationship between the disassembly of the chaperone complex and the progression of the differentiation, the chaperones migrated to the cytoplasm being associated with cytoskeletal rearrangement, whereas the nuclear areas occupied by them in undifferentiated cells become transcriptionally active. In contrast to FKBP52, FKBP51 is not induced during differentiation, remains in the cell body and replaces FKBP52 in the annular structures of the nucleus complexed with hsp70. Importantly, these effects are triggered by FK506 itself without need of other trophic factor.

Initially, it was assumed that the mechanism underlying neurite outgrowth by FK506 was via calcineurin inhibition. However, there were developed a number of ligands lacking immunosuppressant activity that retain the neuroprotective activity (Gold et al. 2005; Voda et al. 2005; Price et al. 2007). It was proposed that the effect of FK506 is mediated by FKBP52 and not by other FKBPs (Gold 1999; Manabe et al. 2002; Price et al. 2005; Kang et al. 2008). Our observations are in line with this hypothesis and also add the fact that FKBP51 seems to antagonize FKBP52 action. It has also been posited that FK506 only works in the presence of neurotrophins. Our experimental evidence shows that FK506 does exert neurotrophic action by itself in both neuroblastoma cells and embryonic hippocampal cells, an effect that seems to be associated with the relocalization of the IMMs and the generation of new protein-protein interactions, some of them essential for the rearrangement of the cytoskeletal architecture. Good examples are the association of p23 with intermediate filaments and the disruption of microtubules and microfilaments in arborization bodies (Fig. 9).

Previous works have related the activation of the MAPK pathway with the mechanism of action of FK506 (Matsuda and Koyasu 2003; Price et al. 2003; Gold and Zhong 2004), although the effect was always mixed with that dependent on neurotrophins. Most of the observations made in our study for FK506-induced differentiation parallel those observed in cells stimulated with cAMP. However it is clear that the events related to cell differentiation do not share the same mechanism.

The ERK cascade is activated during the early steps of differentiation and this activation is linked to the redistribution of chaperones from the nucleus to the cytoplasm (Figs. 6a and 6b). Even though the biochemistry of ERK pathways is well known, how the activation of this pathway achieves different specific responses is unclear. This concept is not only valid for neuronal differentiation, but also for most signaling pathways related to ERK cascade.

The overexpression of FKBP52 induced faster cell differentiation and neurites were longer. The opposite action was observed after knocking-down FKBP52. On the other hand, FKBP51 overexpression decreased both the length of neurites and the rate of cell differentiation, and its knockdown favored neurite outgrowth. FKBP52 (and not FKBP51) concentrates in the growing cones, neurite varicosities that will originate arborization, and the terminal end of axons of neurons or axon-like structures of the cell line.

FKBPs are highly abundant in the nervous system (Snyder et al. 1998). One of the roles recently reported for FKBPs is to interact with proteins belonging to the transient receptor potential channel superfamily (TRPC). The association of FKBP12 and FKBP52 with TRPC channels in rat brain lysates is displaced by FK506 (Sinkins et al. 2004). Since FK506 disrupts both the binding of the IMM to TRPC channels, and it also inhibits the PPIase activity and calcineurin activity, it is unlikely that such inhibitory action of FK506 may be responsible for neuron differentiation, neurite outgrowth and nerve regeneration because all these effects are also seen in FKBP12-KO mice or with FK506 derivatives lacking the ability to activate calcineurin. Our results suggest a more complex network of biological processes in addition to the possible (and tempting) speculation that activity of FKBP52 action may be related to some gating mechanism of those channels. TRPC channels are not exclusive of neurons, but they are widely expressed in several cell types (Parekh and Putney 2005), whereas the effects of FK506 on cell differentiation via hsp90-binding immunophilins are not observed in other tissues and seem to be exclusive for neurons. A good example is shown in Fig. 3e with L1 preadipocytes, a cell line that expresses TRPC channels. It is important to emphasize that the phenomenon described in this study involves an entire rearrangement of neuronal chaperones that may affect simultaneously several aspects of the differentiation physiology, i.e. from gene regulation (Fig. 7) to cytoskeleton organization and axonal growth (Figs. 8, 9 and 11). In this regard, it is likely to postulate that these chaperones may repress gene expression in the annular structures observed in the nucleus of undifferenciated neurons, for example, by favoring the condensation of chromatin. In the cytoplasm, the chaperones acquire a different role influencing the organization of the cytoskeleton, in particular in dendrite bifurcations and terminal axons.

A very recent report has suggested a potential role of IMMs in axon guidance in response to netrin-1 (Shim et al. 2009). Both processes, axon guidance via netrin-1 and the particular rearrangement of the FKBP52•hsp90•p23 complex during the early neuronal differentiation steps, are not directly related since it has also been shown that axons continue to grow after the overexpression of FKBP mutants that blocked the responses to netrin-1, demonstrating that axonal growth was not impaired. Moreover, netrin signaling requires the activity of soluble adenylyl cyclase (Wu et al. 2006), whereas FK506 seems to be independent of this pathway. Rather, our study shows univocally that axonal growth is abrogated according to the balance between FKBP51 and FKBP52, key factors for neuronal differentiation as well.

Recent studies indicates that the periphery of the nucleus provides a platform for sequestering transcription factors away from chromatin when these factors interact physically with components of the inner membrane (Heessen and Fornerod 2007). Additionally, it has been proposed that the nuclear periphery is an epigenetically dynamic compartment containing both active and repressed genes (Luo L 2009). The lamins are developmentally regulated, with all cells expressing B-type lamin, whereas Atype lamins are absent in early embryonic development and in certain stem cell populations in adults (Stewart et al. 2007). This is why we performed the studies of colocalization labeling lamin B. Our findings suggest that the FKBP52•hsp90•p23 complex may shape the nuclear architecture of undifferentiated cells, such that the initiation of the differentiation program promotes the redistribution of the components of the complex, thus affecting gene expression. In line with this hypothesis, pre-mRNA labeling show high and concentrated transcriptional activity in the perinuclear area where the chaperone complex is disassembled before being dispersed in the cytoplasm.

The hsp90-inhibitor radicicol shows some initial effect on neuronal differentiation, but it results toxic in the long term and also impaired FK506 effects (Fig. 1). Previous studies have used hsp90-inhibitors as differentiation agents for neurons, but the stimulation system was a mixture of drug and neurotrophic factors (Gold et al. 1999;Sano et al. 1999). Another important difference was that these studies were performed within a time-frame when inhibitors do not show the deleterious action described in Fig. 1 (Jin and Sano 2008). Because the MEK-ERK-CREB pathway seems to be involved in the FK506-dependent differentiation process (Figs. 1 and 6), one possible candidate to initiate the activation of this cascade is Ras/Raf (Kolch 2000;Pursiheimo et al. 2002;Price et al. 2003). However, the activation of these kinase pathway is entirely dependent on hsp90 (Pratt 1998), so experiments with hsp90 inhibitors such as radicicol or geldanamycin should have prevented neurite outgrowth, which is not the case shown neither here nor by other laboratories. Consequently, FK506 must act down-stream of this pathway.

It has been proposed that the effect of hsp90-inhibitors on the neurite outgrowth may be related to the disruption of steroid receptors (Gold and Villafranca 2003), such that the released chaperone heterocomplex may work via a gain-of-function mechanism. Thus, it was proposed that upon dissociation from the receptor complex, the chaperones may favor retrotransport of signaling endosomes via FKBP52-dynein (Gold 2002) in a similar manner as it has been shown for steroid receptors (Galigniana et al. 2010). However, it should be noted that chaperones are not limiting proteins; actually, they are the most abundant soluble proteins and are greatly induced during the differentiation of neurons (Fig. 1e). Moreover, cells differentiate in the same extend with or without dexamethasone (Figs. 2c and 2d). Even though the influence of non-genomic effects of steroid hormones cannot be ruled out in the long term, the observation that the FKBP52•hsp90•p23 heterocomplex undergoes a dramatic subcellular rearrangement makes more likely that they (FKBP52 in particular) have specific functions on the early steps of the differentiation process. This interpretation is enhanced by the antagonistic action shown by FKBP51, an IMM that shares many structural properties with FKBP52. Therefore, we propose that IMMs are involved in the very early steps of activation of key genes specifically activated during neuronal differentiation and also participate in the rearrangement of the cytoskeleton.

Supplementary Material

Refer to Web version on PubMed Central for supplementary material.

Acknowledgments

This work was supported by grants from Agencia de Promoción Científica y Tecnológica de Argentina (PICT-2006-02109 and PICT-2007-00640), Universidad de Buenos Aires (UBACyT-X085) and the FIRCA Program of the NIH (grants R03TW007162-01A2 and R03TW008143-01A1). We thank Dr. David O. Smith (Mayo Clinic, Scottsdale, AZ, USA) for the kind gift of plasmids encoding for FKBPs.

References

Ayala R, Shu T, Tsai LH. Trekking across the brain: the journey of neuronal migration. Cell. 2007; 128:29–43. [PubMed: 17218253]

Bennett CN, Ross SE, Longo KA, Bajnok L, Hemati N, Johnson KW, Harrison SD, MacDougald OA. Regulation of Wnt signaling during adipogenesis. J Biol Chem. 2002; 277:30998–31004. [PubMed: 12055200]

Buttiglione M, Vitiello F, Sardella E, Petrone L, Nardulli M, Favia P, d'Agostino R, Gristina R. Behaviour of SH-SY5Y neuroblastoma cell line grown in different media and on different chemically modified substrates. Biomaterials. 2007; 28:2932–2945. [PubMed: 17391751]

Castren E. Neurotrophic effects of antidepressant drugs. Curr Opin Pharmacol. 2004; 4:58–64. [PubMed: 15018840]

Colo GP, Rubio MF, Nojek IM, Werbajh SE, Echeverria PC, Alvarado CV, Nahmod VE, Galigniana MD, Costas MA. The p160 nuclear receptor co-activator RAC3 exerts an anti-apoptotic role through a cytoplasmatic action. Oncogene. 2008; 27:2430–2444. [PubMed: 17968310]

Consales C, Volpicelli F, Greco D, Leone L, Colucci-D'Amato L, Perrone-Capano C, di Porzio U. GDNF signaling in embryonic midbrain neurons in vitro. Brain Res. 2007; 1159:28–39. [PubMed: 17574220]

Czar MJ, Welsh MJ, Pratt WB. Immunofluorescence localization of the 90-kDa heat-shock protein to cytoskeleton. Eur J Cell Biol. 1996; 70:322–330. [PubMed: 8864660]

Chambraud B, Belabes H, Fontaine-Lenoir V, Fellous A, Baulieu EE. The immunophilin FKBP52 specifically binds to tubulin and prevents microtubule formation. Faseb J. 2007; 21:2787–2797. [PubMed: 17435176]

Cheung-Flynn J, Prapapanich V, Cox MB, Riggs DL, Suarez-Quian C, Smith DF. Physiological role for the cochaperone FKBP52 in androgen receptor signaling. Mol Endocrinol. 2005; 19:1654–1666. [PubMed: 15831525]

Echeverria PC, Mazaira G, Erlejman A, Gomez-Sanchez C, Piwien Pilipuk G, Galigniana MD. Nuclear import of the glucocorticoid receptor-hsp90 complex through the nuclear pore complex is mediated by its interaction with Nup62 and importin beta. Mol Cell Biol. 2009; 29:4788–4797. [PubMed: 19581287]

Encinas M, Iglesias M, Liu Y, Wang H, Muhaisen A, Cena V, Gallego C, Comella JX. Sequential treatment of SH-SY5Y cells with retinoic acid and brain-derived neurotrophic factor gives rise to fully differentiated, neurotrophic factor-dependent, human neuron-like cells. J Neurochem. 2000; 75:991–1003. [PubMed: 10936180]

Freeman BC, Felts SJ, Toft DO, Yamamoto KR. The p23 molecular chaperones act at a late step in intracellular receptor action to differentially affect ligand efficacies. Genes Dev. 2000; 14:422–434. [PubMed: 10691735]

Galigniana MD. Native rat kidney mineralocorticoid receptor is a phosphoprotein whose transformation to a DNA-binding form is induced by phosphatases. Biochem J. 1998; 333 (Pt 3): 555–563. [PubMed: 9677313]

Galigniana MD, Echeverría PC, Erlejman AG, Piwien-Pilipuk G. Role of molecular chaperones and TPR-domain proteins in the cytoplasmic transport of steroid receptors and their passage through the nuclear pore. Nucleus. 2010; 1:299–308. [PubMed: 21113270]

Galigniana MD, Radanyi C, Renoir JM, Housley PR, Pratt WB. Evidence that the peptidylprolyl isomerase domain of the hsp90-binding immunophilin FKBP52 is involved in both dynein interaction and glucocorticoid receptor movement to the nucleus. J Biol Chem. 2001; 276:14884–14889. [PubMed: 11278753]

Galigniana MD, Harrell JM, O'Hagen HM, Ljungman M, Pratt WB. Hsp90-binding immunophilins link p53 to dynein during p53 transport to the nucleus. J Biol Chem. 2004a; 279:22483–22489. [PubMed: 15004035]

Galigniana MD, Harrell JM, Housley PR, Patterson C, Fisher SK, Pratt WB. Retrograde transport of the glucocorticoid receptor in neurites requires dynamic assembly of complexes with the protein chaperone hsp90 and is linked to the CHIP component of the machinery for proteasomal degradation. Brain Res Mol Brain Res. 2004b; 123:27–36. [PubMed: 15046863]

Galigniana MD, Scruggs JL, Herrington J, Welsh MJ, Carter-Su C, Housley PR, Pratt WB. Heat shock protein 90-dependent (geldanamycin-inhibited) movement of the glucocorticoid receptor through the cytoplasm to the nucleus requires intact cytoskeleton. Mol Endocrinol. 1998; 12:1903–1913. [PubMed: 9849964]

Galigniana MD, Harrell JM, Murphy PJ, Chinkers M, Radanyi C, Renoir JM, Zhang M, Pratt WB. Binding of hsp90-associated immunophilins to cytoplasmic dynein: direct binding and in vivo evidence that the peptidylprolyl isomerase domain is a dynein interaction domain. Biochemistry. 2002; 41:13602–13610. [PubMed: 12427021]

Gallo LI, Ghini AA, Pilipuk GP, Galigniana MD. Differential recruitment of tetratricorpeptide repeat domain immunophilins to the mineralocorticoid receptor influences both heat-shock protein 90-dependent retrotransport and hormone-dependent transcriptional activity. Biochemistry. 2007; 46:14044–14057. [PubMed: 18001136]

Gkika D, Topala CN, Hoenderop JG, Bindels RJ. The immunophilin FKBP52 inhibits the activity of the epithelial Ca2+ channel TRPV5. Am J Physiol Renal Physiol. 2006; 290:F1253–1259. [PubMed: 16352746]

Gold, B. Neuroimmunophilin ligands and the role of steroid hormone chaperone proteins in nerve regeneration. In: Gold, BFG.; Herdegen, T., editors. Immunophilins in the Brain. FKBP-ligands: Novel strategies for the treatment of neurodegenerative disorders. Prous Science; Barcelona: 2000. p. 3-22.

Gold B. Immunophilin ligands in nerve regeneration. Science & Medicine. 2002; 8:66–75.

Gold BG. FK506 and the role of the immunophilin FKBP-52 in nerve regeneration. Drug Metab Rev. 1999; 31:649–663. [PubMed: 10461545]

Gold BG, Villafranca JE. Neuroimmunophilin ligands: the development of novel neuroregenerative/neuroprotective compounds. Curr Top Med Chem. 2003; 3:1368–1375. [PubMed: 12871168]

Gold BG, Zhong YP. FK506 requires stimulation of the extracellular signal-regulated kinase 1/2 and the steroid receptor chaperone protein p23 for neurite elongation. Neurosignals. 2004; 13:122–129. [PubMed: 15067199]

Gold BG, Armistead DM, Wang MS. Non-FK506-binding protein-12 neuroimmunophilin ligands increase neurite elongation and accelerate nerve regeneration. J Neurosci Res. 2005; 80:56–65. [PubMed: 15732051]

Gold BG, Densmore V, Shou W, Matzuk MM, Gordon HS. Immunophilin FK506-binding protein 52 (not FK506-binding protein 12) mediates the neurotrophic action of FK506. J Pharmacol Exp Ther. 1999; 289:1202–1210. [PubMed: 10336507]

Hansen TO, Rehfeld JF, Nielsen FC. KCl potentiates forskolin-induced PC12 cell neurite outgrowth via protein kinase A and extracellular signal-regulated kinase signaling pathways. Neurosci Lett. 2003; 347:57–61. [PubMed: 12865141]

Heessen S, Fornerod M. The inner nuclear envelope as a transcription factor resting place. EMBO Rep. 2007; 8:914–919. [PubMed: 17906672]

Hu HJ, Glauner KS, Gereau RWt. ERK integrates PKA and PKC signaling in superficial dorsal horn neurons. I. Modulation of A-type K+ currents. J Neurophysiol. 2003; 90:1671–1679. [PubMed: 12750419]

Inberg A, Bogoch Y, Bledi Y, Linial M. Cellular processes underlying maturation of P19 neurons: Changes in protein folding regimen and cytoskeleton organization. Proteomics. 2007; 7:910–920. [PubMed: 17370269]

Jackson DA, Hassan AB, Errington RJ, Cook PR. Visualization of focal sites of transcription within human nuclei. Embo J. 1993; 12:1059–1065. [PubMed: 8458323]

Jin E, Sano M. Neurite outgrowth of NG108-15 cells induced by heat shock protein 90 inhibitors. Cell Biochem Funct. 2008; 26:825–832. [PubMed: 18636417]

Kang CB, Hong Y, Dhe-Paganon S, Yoon HS. FKBP family proteins: immunophilins with versatile biological functions. Neurosignals. 2008; 16:318–325. [PubMed: 18635947]

Kolch W. Meaningful relationships: the regulation of the Ras/Raf/MEK/ERK pathway by protein interactions. Biochem J. 2000; 351(Pt 2):289–305. [PubMed: 11023813]

Kosano H, Stensgard B, Charlesworth MC, McMahon N, Toft D. The assembly of progesterone receptor-hsp90 complexes using purified proteins. J Biol Chem. 1998; 273:32973–32979. [PubMed: 9830049]

Luo LGK, Petell LM, Wilson CL, Bewersdorf J, Shopland LS. The nuclear periphery of embryonic stem cells is a transcriptionally permissive and repressive compartment. J Cell Sci. 2009; 122:3729–3737. [PubMed: 19773359]

Manabe Y, Warita H, Murakami T, Shiote M, Hayashi T, Omori N, Nagano I, Shoji M, Abe K. Early decrease of the immunophilin FKBP 52 in the spinal cord of a transgenic model for amyotrophic lateral sclerosis. Brain Res. 2002; 935:124–128. [PubMed: 12062482]

Matsuda S, Koyasu S. Regulation of MAPK signaling pathways through immunophilin-ligand complex. Curr Top Med Chem. 2003; 3:1358–1367. [PubMed: 12871167]

Murphy PJ, Morishima Y, Chen H, Galigniana MD, Mansfield JF, Simons SS Jr, Pratt WB. Visualization and mechanism of assembly of a glucocorticoid receptor.Hsp70 complex that is primed for subsequent Hsp90-dependent opening of the steroid binding cleft. J Biol Chem. 2003; 278:34764–34773. [PubMed: 12807878]

Parekh AB, Putney JW Jr. Store-operated calcium channels. Physiol Rev. 2005; 85:757–810. [PubMed: 15788710]

Piwien Pilipuk G, Vinson GP, Sanchez CG, Galigniana MD. Evidence for NL1-Independent Nuclear Translocation of the Mineralocorticoid Receptor. Biochemistry. 2007; 46:1389–1397. [PubMed: 17260968]

Pratt WB. The hsp90-based chaperone system: involvement in signal transduction from a variety of hormone and growth factor receptors. Proc Soc Exp Biol Med. 1998; 217:420–434. [PubMed: 9521088]

Pratt WB, Galigniana MD, Harrell JM, DeFranco DB. Role of hsp90 and the hsp90-binding immunophilins in signalling protein movement. Cell Signal. 2004a; 16:857–872. [PubMed: 15157665]

Pratt WB, Galigniana MD, Morishima Y, Murphy PJ. Role of molecular chaperones in steroid receptor action. Essays Biochem. 2004b; 40:41–58. [PubMed: 15242338]

Price RD, Yamaji T, Matsuoka N. FK506 potentiates NGF-induced neurite outgrowth via the Ras/Raf/MAP kinase pathway. Br J Pharmacol. 2003; 140:825–829. [PubMed: 14559856]

Price RD, Milne SA, Sharkey J, Matsuoka N. Advances in small molecules promoting neurotrophic function. Pharmacol Ther. 2007; 115:292–306. [PubMed: 17599430]

Price RD, Yamaji T, Yamamoto H, Higashi Y, Hanaoka K, Yamazaki S, Ishiye M, Aramori I, Matsuoka N, Mutoh S, Yanagihara T, Gold BG. FK1706, a novel non-immunosuppressive immunophilin: neurotrophic activity and mechanism of action. Eur J Pharmacol. 2005; 509:11–19. [PubMed: 15713424]

Pursiheimo JP, Kieksi A, Jalkanen M, Salmivirta M. Protein kinase A balances the growth factor-induced Ras/ERK signaling. FEBS Lett. 2002; 521:157–164. [PubMed: 12067709]

Ratajczak T, Carrello A. Cyclophilin 40 (CyP-40), mapping of its hsp90 binding domain and evidence that FKBP52 competes with CyP-40 for hsp90 binding. J Biol Chem. 1996; 271:2961–2965. [PubMed: 8621687]

Roche FK, Marsick BM, Letourneau PC. Protein synthesis in distal axons is not required for growth cone responses to guidance cues. J Neurosci. 2009; 29:638–652. [PubMed: 19158291]

Sano M, Yoshida M, Fukui S, Kitajima S. Radicicol potentiates neurotrophin-mediated neurite outgrowth and survival of cultured sensory neurons from chick embryo. J Neurochem. 1999; 72:2256–2263. [PubMed: 10349833]

Santos SD, Verveer PJ, Bastiaens PI. Growth factor-induced MAPK network topology shapes Erk response determining PC-12 cell fate. Nat Cell Biol. 2007; 9:324–330. [PubMed: 17310240]

Schirmer EC, Foisner R. Proteins that associate with lamins: many faces, many functions. Exp Cell Res. 2007; 313:2167–2179. [PubMed: 17451680]

Shim S, Yuan JP, Kim JY, Zeng W, Huang G, Milshteyn A, Kern D, Muallem S, Ming GL, Worley PF. Peptidyl-prolyl isomerase FKBP52 controls chemotropic guidance of neuronal growth cones via regulation of TRPC1 channel opening. Neuron. 2009; 64:471–483. [PubMed: 19945390]

Shu T, Ayala R, Nguyen MD, Xie Z, Gleeson JG, Tsai LH. Ndel1 operates in a common pathway with LIS1 and cytoplasmic dynein to regulate cortical neuronal positioning. Neuron. 2004; 44:263–277. [PubMed: 15473966]

Sinars CR, Cheung-Flynn J, Rimerman RA, Scammell JG, Smith DF, Clardy J. Structure of the large FK506-binding protein FKBP51, an Hsp90-binding protein and a component of steroid receptor complexes. Proc Natl Acad Sci U S A. 2003; 100:868–873. [PubMed: 12538866]

Sinkins WG, Goel M, Estacion M, Schilling WP. Association of immunophilins with mammalian TRPC channels. J Biol Chem. 2004; 279:34521–34529. [PubMed: 15199065]

Snyder SH, Lai MM, Burnett PE. Immunophilins in the nervous system. Neuron. 1998; 21:283–294. [PubMed: 9728910]

Stewart CL, Kozlov S, Fong LG, Young SG. Mouse models of the laminopathies. Exp Cell Res. 2007; 313:2144–2156. [PubMed: 17493612]

Sullivan WP, Owen BA, Toft DO. The influence of ATP and p23 on the conformation of hsp90. J Biol Chem. 2002; 277:45942–45948. [PubMed: 12324468]

Tolstonog GV, Sabasch M, Traub P. Cytoplasmic intermediate filaments are stably associated with nuclear matrices and potentially modulate their DNA-binding function. DNA Cell Biol. 2002; 21:213–239. [PubMed: 12015898]

Tucker RP. The roles of microtubule-associated proteins in brain morphogenesis: a review. Brain Res Brain Res Rev. 1990; 15:101–120. [PubMed: 2282447]

Voda J, Yamaji T, Gold BG. Neuroimmunophilin ligands improve functional recovery and increase axonal growth after spinal cord hemisection in rats. J Neurotrauma. 2005; 22:1150–1161. [PubMed: 16238491]

Wang X, Pongrac JL, DeFranco DB. Glucocorticoid receptors in hippocampal neurons that do not engage proteasomes escape from hormone-dependent down-regulation but maintain transactivation activity. Mol Endocrinol. 2002; 16:1987–1998. [PubMed: 12198236]

Willard MD, Willard FS, Li X, Cappell SD, Snider WD, Siderovski DP. Selective role for RGS12 as a Ras/Raf/MEK scaffold in nerve growth factor-mediated differentiation. Embo J. 2007; 26:2029–2040. [PubMed: 17380122]

Wochnik GM, Ruegg J, Abel GA, Schmidt U, Holsboer F, Rein T. FK506-binding proteins 51 and 52 differentially regulate dynein interaction and nuclear translocation of the glucocorticoid receptor in mammalian cells. J Biol Chem. 2005; 280:4609–4616. [PubMed: 15591061]

Wu KY, Zippin JH, Huron DR, Kamenetsky M, Hengst U, Buck J, Levin LR, Jaffrey SR. Soluble adenylyl cyclase is required for netrin-1 signaling in nerve growth cones. Nat Neurosci. 2006; 9:1257–1264. [PubMed: 16964251]

Xiao L, Chen Y. Culture condition and embryonic stage dependent silence of glucocorticoid receptor expression in hippocampal neurons. J Steroid Biochem Mol Biol. 2008; 111:147–155. [PubMed: 18625317]

Xiao L, Qi A, Chen Y. Cultured embryonic hippocampal neurons deficient in glucocorticoid (GC) receptor: a novel model for studying nongenomic effects of GC in the neural system. Endocrinology. 2005; 146:4036–4041. [PubMed: 15961565]

Yang YJ, Lee HJ, Choi DH, Huang HS, Lim SC, Lee MK. Effect of scoparone on neurite outgrowth in PC12 cells. Neurosci Lett. 2008; 440:14–18. [PubMed: 18547723]

Yao H, York RD, Misra-Press A, Carr DW, Stork PJ. The cyclic adenosine monophosphate-dependent protein kinase (PKA) is required for the sustained activation of mitogen-activated kinases and gene expression by nerve growth factor. J Biol Chem. 1998; 273:8240–8247. [PubMed: 9525930]

Zhao W, Zhong L, Wu J, Chen L, Qing K, Weigel-Kelley KA, Larsen SH, Shou W, Warrington KH Jr, Srivastava A. Role of cellular FKBP52 protein in intracellular trafficking of recombinant adeno-associated virus 2 vectors. Virology. 2006; 353:283–293. [PubMed: 16828834]

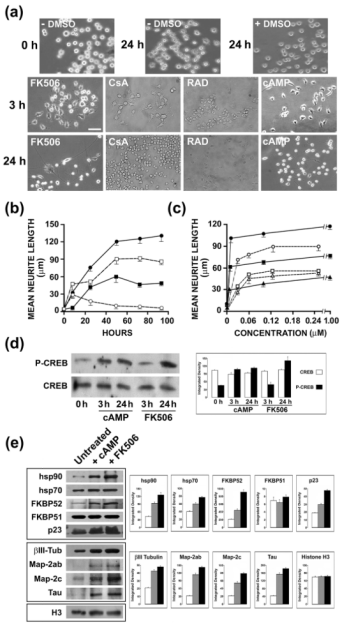

Fig. 1.

Stimulation for neurite outgrowth. (a) Undifferentiated neuroblastoma N2a cells were incubated in DMEM medium supplemented only with 1 μM tacrolimus (*FK506*), 10 nM cyclosporine A, (*CsA*), 0.2 μM radicicol (*RAD*), 125 μM dibutyryl-cAMP, or 0.1% v/v vehicle (*DMSO*). Bar= 40 μm. (b) Neurite outgrowth kinetics. Undifferentiated cells were incubated for the indicated times with either 100 nM FK506 (●), 125 μM dibutyryl-cAMP (□), 0.2 μM radicicol (■) or 10 nM cyclosporine A (○). Results represent the mean ± S.D. for more than 100 cells. (c) Comparative concentration-response curves for the most active drugs. Neurite length was measured in function of the concentration of FK506 (close symbols) or dibutyryl-cAMP (open symbols) after 3 h (triangles), 24 h (squares) or 48 h (circles). Results are the mean ± S.D. for more than 100 cells. (d) Western blot for the induction of CREB phosphorylation upon cell treatment for 3 h and 24 h with 125 μM dibutyryl-cAMP or 1 μM FK506 in a serum-free medium. Bar graphs show the optical density of the Western blots (mean ± S.D, n=3). (e) Induction of chaperones and neuronal markers. Cells were incubated in the absence (*Untreated*) or presence of 125 μM dibutyryl-cAMP (+*cAMP*) or 1 μM FK506 (+*FK506*). Histone H3 was used as loading control. Bar graphs show the optical density of the Western blots (*white*: untreated cells, *gray*: cAMP-treated cells, *black*: FK506-treated cells).

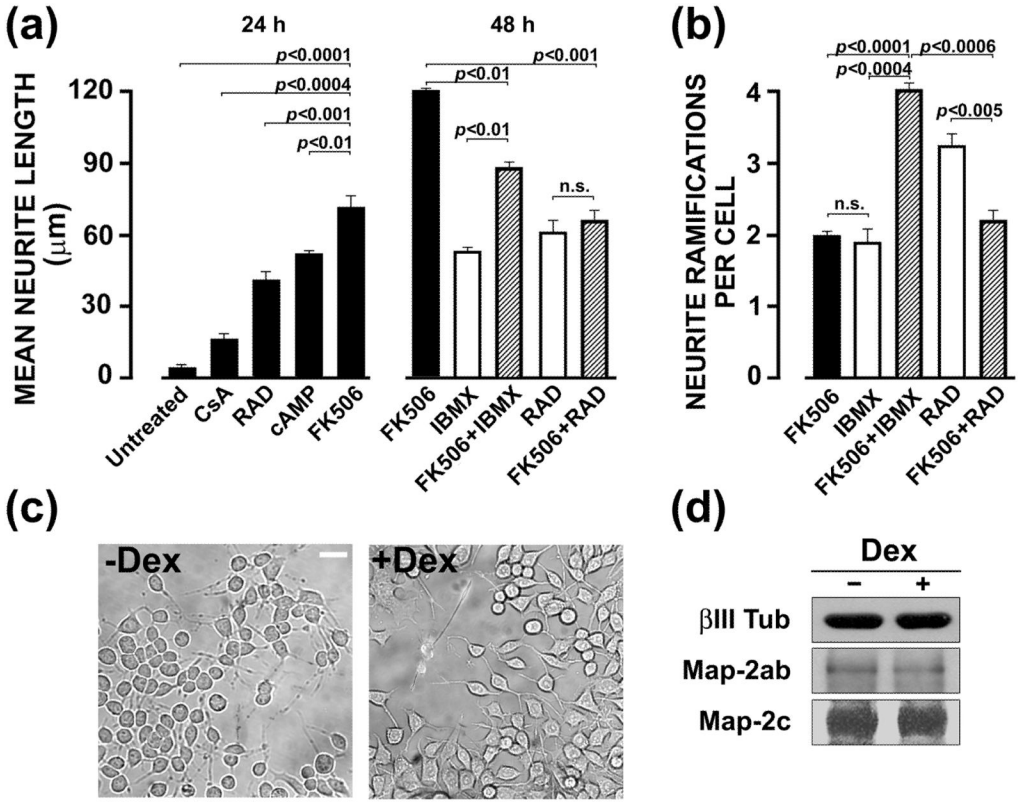

Fig. 2.

Effect of combined treatments on neurite outgrowth. (a) Neurite length was measured for treatments with individual or combined drugs at the concentrations used in Fig. 1*C*. (b) Number of ramifications per cell. (c) Effect of glucocorticoids on cell differentiation. N2a cells were preincubated for 24 h in DMEM/5% charcoal-stripped serum and then, induced to differentiate for 24 h with 1 μM FK506 with 1 μM dexamethasone (+Dex) or 0.1% vehicle (−Dex). Bar = 25 μM. (d) Cell lysates of dexamethasone-treated cells were Western blotted for βIII-tubulin and Map-2a, Map-2b, and Map-2c.

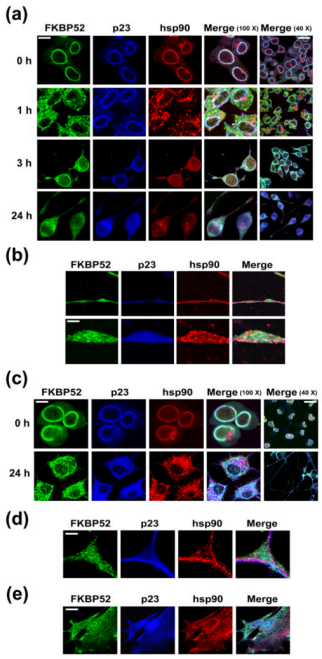

Fig. 3.

Subcellular localization of FKBP52, hsp90 and p23 in N2a cells. (a) Images by confocal microscopy of undifferentiated cells prior (0 h) or after (3 h and 24 h) of treatment with FK506. Image on the right hand shows a wider field. (b) The upper panel shows the distribution of proteins in an axon-like structure; the lower panel shows a magnification of a ramification body. Note the central distribution of FKBP52 with respect to hsp90 and p23. (c) Subcellular localization of FKBP52, hsp90 and p23 in embryonic hippocampal cells (day 17) treated for 24 with 1 μM FK506 or vehicle. Image on the right hand shows a wider field. (d) Subcellular distribution of proteins in axons. Note the central distribution of FKBP52 with respect to hsp90 and p23. (e) Undifferentiated L1 preadipocytes do not show annular structures. Bars on the upper left corner of panels a, c and e (100 × magnification)= 10 μm. Bars on on the upper right corner of panels a and c (40 × magnification) = 25 μm. Bars on panels b and d = 2.5 μm

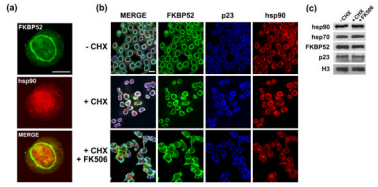

Fig. 4.

The annular ring of chaperones is a preassembled structure. (a) Undifferentiated N2a cells were stained with the Ac88 clone anti-hsp90 (red), which does not recognize the chaperone unless it is free or denatured. FKBP52 was used as marker of the perinuclear ring (green). (b) Indirect immunofluorescence for N2a cells preincubated for 30 min with cycloheximide (+ CHX) followed by stimulation with FK506 for 3 h (+ CHX + FK506) without changing the medium. (− CHX): Control of untreated cells. Bars = 10 μm.

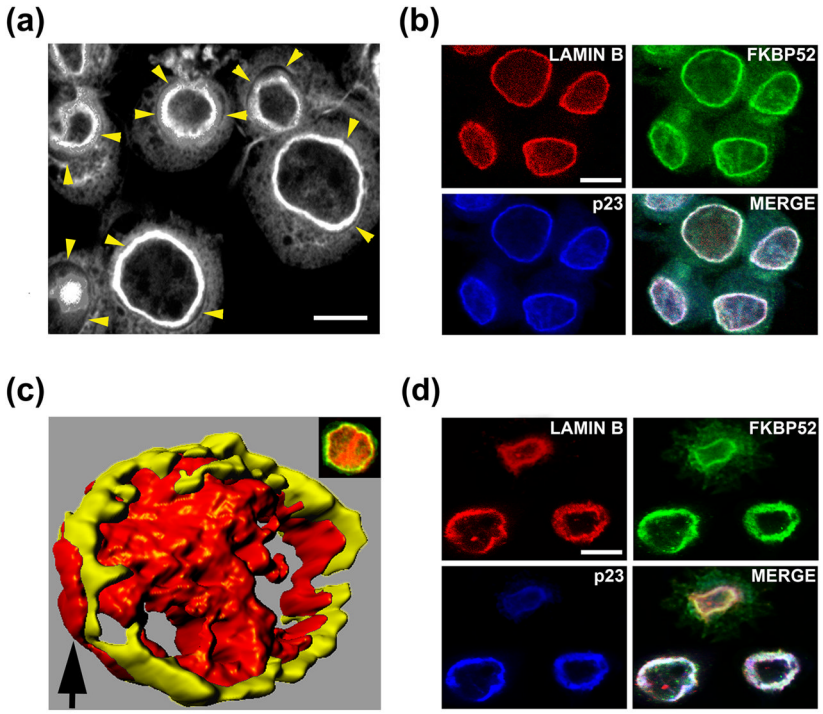

Fig. 5.

Confocal microscopy images show that the annular distribution of the FKBP52•hsp90•p23 complex is intranuclear (a) The borders of nuclei (pointed by yellow arrow-heads) are shown compared with the annular structure. (b) Indirect immunofluorescence for B-type lamin (red), FKBP52 (green) and p23 (blue). (c) Computer generated 3-D image of a cell immunostained for p23 (green) whose nucleus was stained with TO-PRO-3 iodine (insert). The black arrow shows a portion of chromatin surrounding the annular structure. White bars = 10 μm.

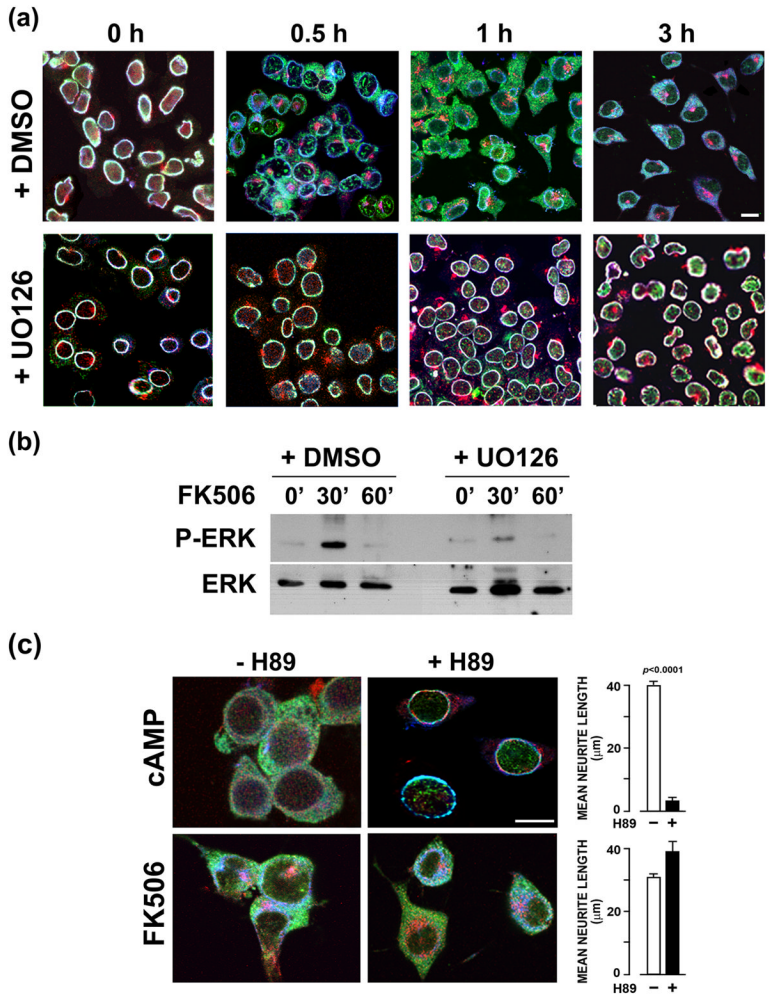

Fig. 6.

ERK activation relates to the subcellular rearrangement of chaperones. (a) N2a cells were maintained in serum-free medium for 18 h and preincubated with 10 μM UO126 (or vehicle) for 30 min. Cells were incubated with 1 μM FK506, fixed after 0.5, 1 and 3 hours, and immunosatined for hsp90 (red), FKBP52 (green) and p23 (blue). Bar = 10 μm. (b) Western blots of whole cell lysates shown the effectiveness of the treatment with the MEK inhibitor. (c) PKA inhibitor H89 prevents neurite outgrowth and chaperone disassembly in cells stimulated to differentiate with 60 μM dibutyryl-cAMP, but it is ineffective with cells treated with 1 μM FK506. Cells were starved of serum for 3 h, preincubated with H89 for 40 min, and then incubated with the differentiation agent for 3 h. Bar = 10 μm.

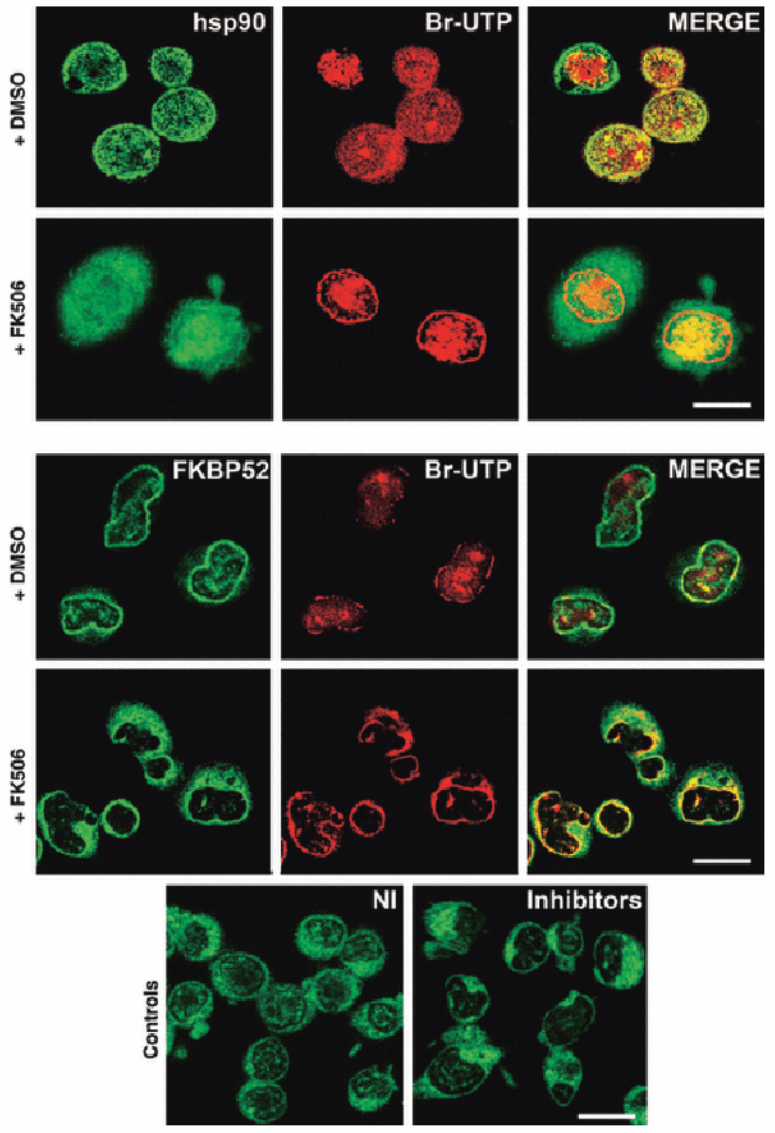

Fig. 7.

The perinuclear ring becomes transcriptionally active with FK506. Note the ring of Br-UTP when hsp90 and FKBP52 spread out in the cytoplasm after 3 h treatment. The lower panels show controls for Br-uridine staining in FK506-treated cells incubated with a non-immune IgG (*NI*) rather than the anti-Br-uridine IgG, and cells where transcriptional activity was inhibited with α-amanitin and actinomycin D (*Inhibitors*). The green background corresponds to the anti-FKBP52 antibody signal. Bars= 10 μm.

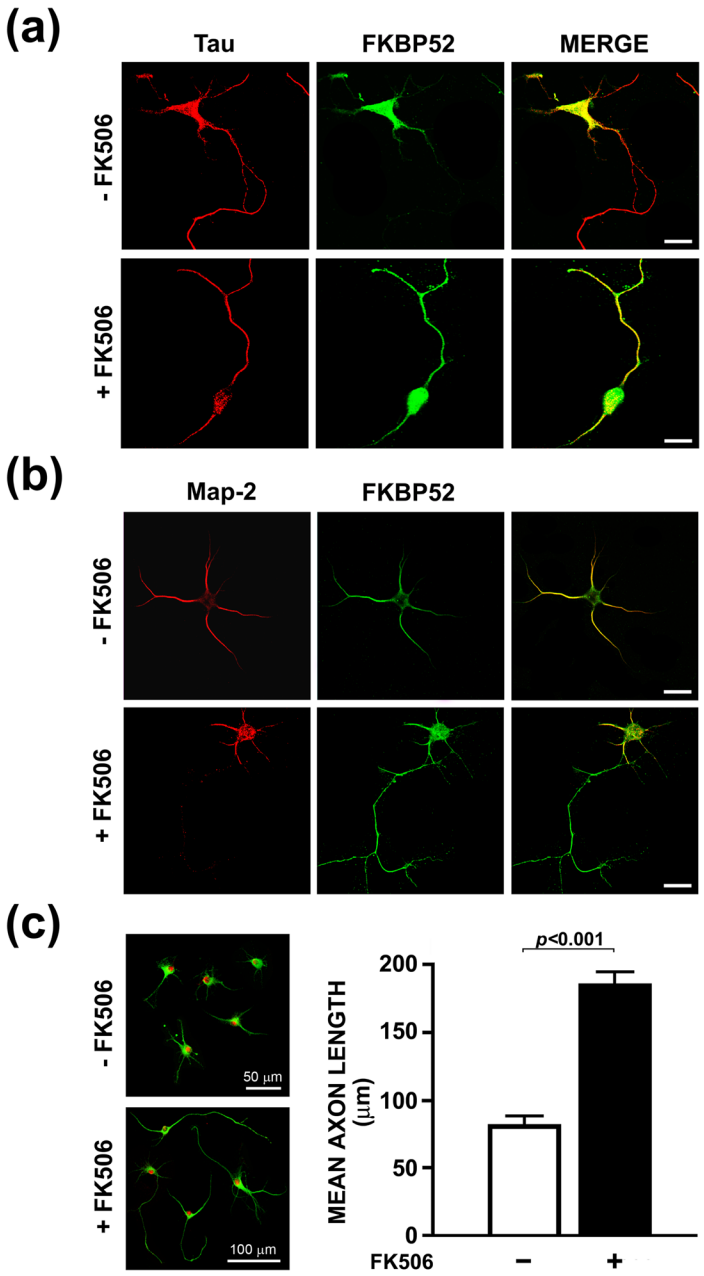

Fig. 8.

FKBP52 concentrates in axons of embryonic hippocampal neurons treated for 24 h with 1 μM FK506. (a) Indirect immunofluorescence for the axonal marker Tau-1 and FKBP52 in cells cultured for 3 days. (b) Indirect immunofluorescence for the dendrite marker Map-2 and FKBP52 in cells cultured for 7 days. (c) Primary hippocampal cells cultured for 3 days with FK506 show significantly longer axons than untreated neurons. Bars in panels (a) and (b) = 40 μm.

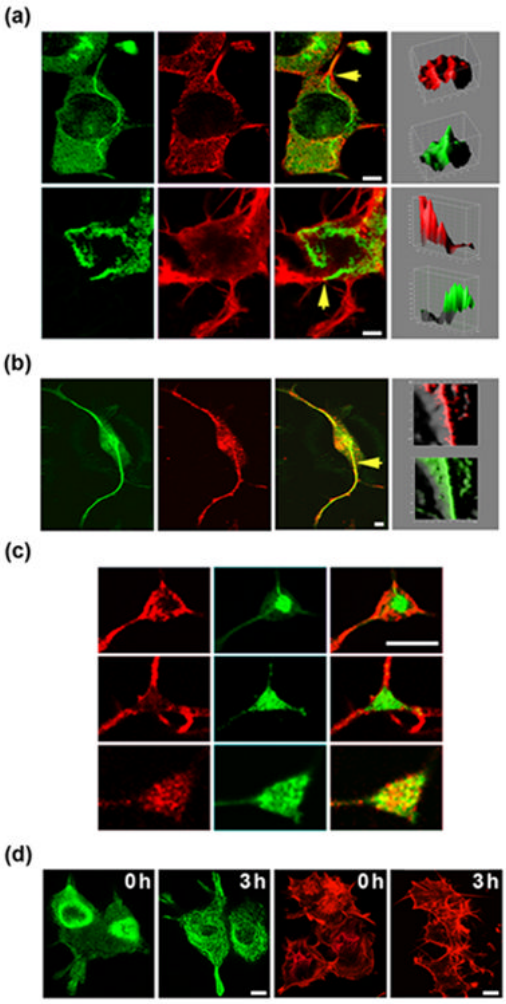

Fig. 9.

Cytoskeletal rearrangement. Cells were differentiated with FK506 for 3 h, fixed and stained for (a) p23 (green) and microtubules (upper cell) and microfilaments (lower cell). or (b) intermediate filaments. On the right hand side it is shown the 3D-surface plot profile for each protein at the level of the arrow-head. (c) Magnified image of arborization bodies shown the disruption of microtubules (upper) and microfilaments (middle) but not intermediate filaments (lower) where p23 (shown in green) is concentrated. (d) Microtubule staining (green) and microfilament staining (red) for undifferentiated cells (0 h) and FK506-treated cells (3 h). Note the expected filamentary pattern of microtubules is almost absent in the undifferentiated cells. All bars = 10 μm.

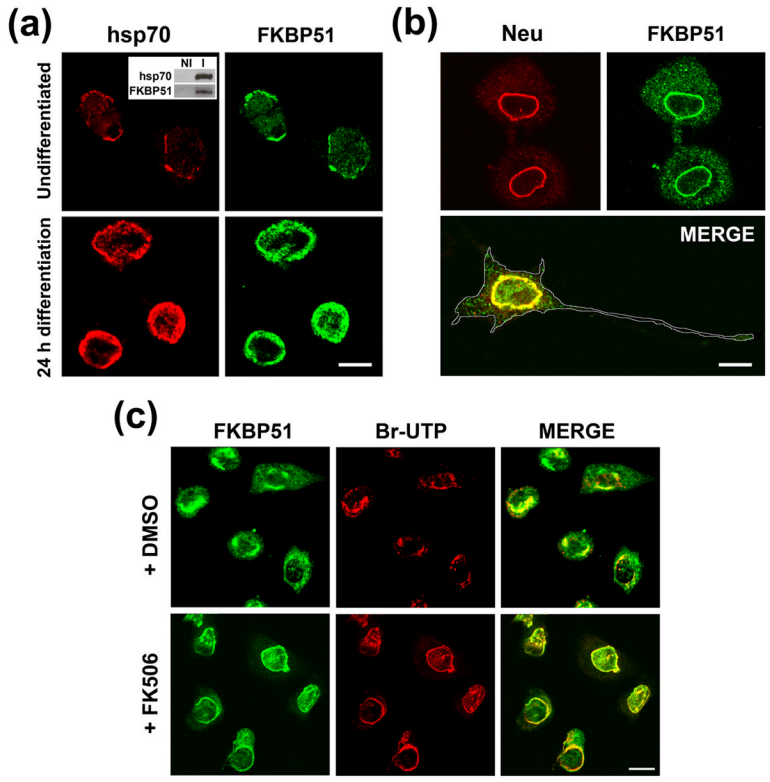

Fig. 10.

Nuclear swapping of immunophilins. (a) Confocal images for hsp70 and FKBP51 in N2a cells treated or not with 1 μM FK506 for 24 h. The insert shows the coimmunoprecipitation of FKBP51 with hsp70 (NI: non-immune IgG, I: anti-hsp70 IgG. (b) Confocal images for neurofilaments (Neu) and FKP51 in cells treated with FK506 for 24 h. The lower cell shows the lack of localization of FKBP51 in the axon. (c) FKBP51 concentrates in transcriptionally active nuclear domains. Cells were treated with FK506 for 6 h and pre-mRNAs were labeled with Br-UTP as described for Fig. 7. FKBP51 and FKP52 were visualized by indirect immunofluorescence. Bars= 10 μm

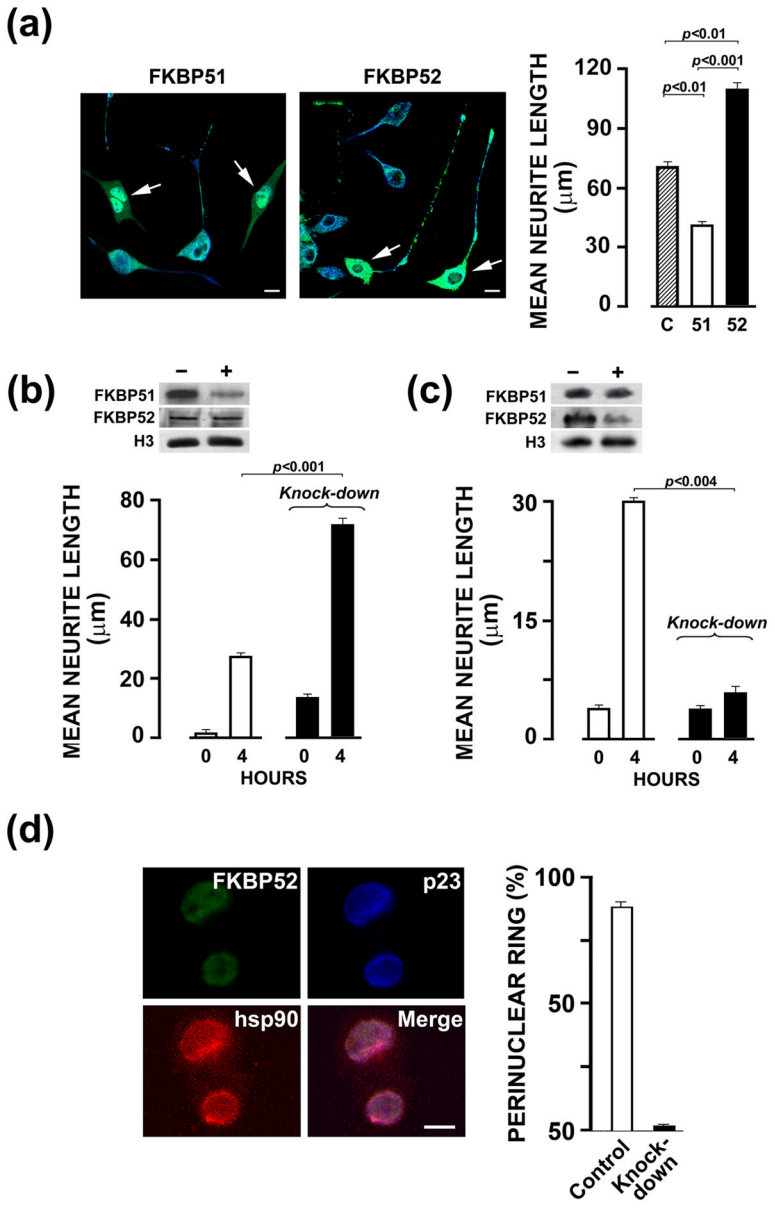

Fig. 11.

FKBP51 antagonizes FKBP52-dependent neurite outgrowth. (a) N2a cells were transfected with FKBP51 or FKBP52 and stimulated with FK506. Cells were fixed and stained for each IMM (green) and p23 (blue). Neurite length was measured in cells overexpressing the IMM (mostly green cells pointed by arrows) or not (mostly turquoise-blue cells). The bar graph on the right hand shows that, compared to untransfected control cells (C, hatched bar), neurite length is larger in cells overexpressing FKBP52 (52, black bar) and shorter in cells overexpressing FKBP51 (51, white bar). (b) Knock-down of FKBP51 (black bars) favors neurite outgrowth respect to control cells (white bars) after 4 h of treatment with FK506. The Western blot shows that FKBP52 expression is not affected by knocking-down FKBP51. H3: histone H3 used as loading control. (c) Identical experiment as in the previous panel but knocking-down FKBP52. (d) The image shows the zero time for untransformed cells where the expression of FKBP52 was knocked-down. Note the lack of the prominent perinuclear ring observed in the regular cells (a quantification is shown in the bar graph).

The green channel was overexposed to permit the visualization of the minimal expression of FKBP52. Bar = 10 μm.